

**4'-(Pyrimidin-5-yl)- and 4'-(2-methylpyrimidin-5-yl)-
4,2':6',4''-terpyridines: selective coordination to zinc(II)
through the 4,2':6',4''-terpyridine domain**

**Y. Maximilian Klein, Edwin C. Constable, Catherine E. Housecroft* and Jennifer
A. Zampese**

Department of Chemistry, University of Basel, Spitalstrasse 51, 4056-Basel, Switzerland

Fax: +41 61 267 1018; E-mail: catherine.housecroft@unibas.ch

Abstract

The preparation and characterization of the compounds 4'-(pyrimidin-5-yl)-4,2':6',4''-terpyridine (**3**) and 4'-(2-methylpyrimidin-5-yl)-4,2':6',4''-terpyridine (**4**) are described. Preferential coordination through the terminal pyridine donors of the tpy domain is observed when **3** and **4** are treated with ZnCl₂ or ZnI₂. The 1-dimensional coordination polymers [$\{\text{ZnCl}_2(\mathbf{3})\}_n$], [$\{\text{ZnI}_2(\mathbf{3})\}_n$] and [$\{\text{ZnI}_2(\mathbf{4})\cdot\text{MeOH}\}_n$] have been structurally characterized by single crystal X-ray crystallography. [$\{\text{ZnI}_2(\mathbf{3})\}_n$] is helical and crystallizes with both *P*- and *M*-helices in the lattice; the packing of *P*- and *M*-chains involves discrete tetradecamer π -stacking domains involving 4,2':6',4''-tpy units. The introduction of the 2-methyl substituent on going from **3** to **4** has only a small effect on the structure of [$\{\text{ZnI}_2(\text{L})\}_n$] (L = **3** or **4**). The two coordination polymer chains assemble through face-to-face π -interactions into sheets with the pyrimidin-5-yl units projecting outwards. The presence of the 2-methyl substituents in **4** forces the sheets in

$[\{\text{ZnI}_2(\mathbf{4})\cdot\text{MeOH}\}_n]$ further apart compared to those in $[\{\text{ZnI}_2(\mathbf{3})\}_n]$, leading to the accommodation of MeOH molecules in cavities between the sheets.

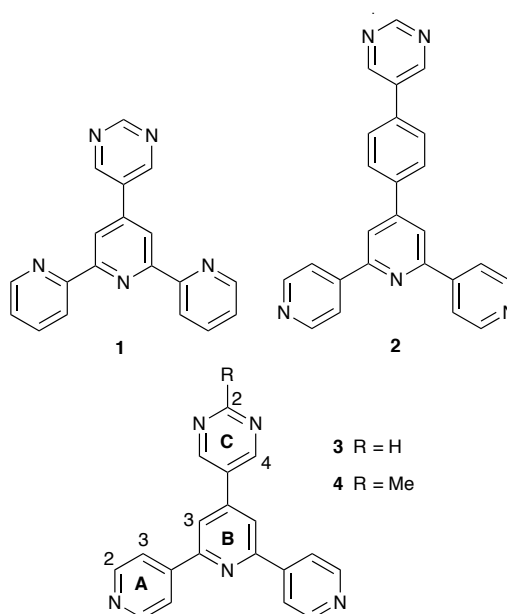
Keywords: 4,2':6',4''-terpyridine; zinc; structure; coordination polymer; X-ray diffraction

1. Introduction

The use of 4,2':6',4''-terpyridine (4,2':6',4''-tpy) ligands as metal-binding domains for the assembly of coordination polymers is highly attractive and topical [1]. Of the three nitrogen donors in 4,2':6',4''-tpy, only the outer two typically bind metal ions leading to a divergent, V-shaped building block with well-defined directionality. The reaction of 4,2':6',4''-tpy with ZnCl_2 leads to a helical coordination polymer $[\{\text{ZnCl}_2(4,2':6',4''\text{-tpy})_n]$ [2], and this structural motif persists in a range of $[\{\text{ZnX}_2(4'\text{-R-}4,2':6',4''\text{-tpy})_n]$ polymers in which R is a *tert*-butyl [3], aryl [4,5] or 4-alkoxyphenyl [6] substituent. Coordinatively non-innocent 4'-R functionalities have the potential to extend the coordination assembly and examples include a closed metallocapsule when R = 4-pyridyl [7,8] and 2- or 3- dimensional networks when R = CO_2H [9,10,11]. We have also recently illustrated the assembly of a 2D \rightarrow 2D parallel interpenetrated array of (4,4) sheets by using a ditopic bis(4,2':6',4''-terpyridine) [12].

We have previously demonstrated that the 2,2':6',2''-tpy domain in ligand **1** (Scheme 1) preferentially binds iron(II) or ruthenium(II) leaving the 5-pyrimidyl substituent as a pendant moiety in the discrete complex cations $[\text{Fe}(\mathbf{1})_2]^{2+}$ and $[\text{Ru}(\mathbf{1})_2]^{2+}$ [13]. Post-treatment of $[\text{Ru}(\mathbf{1})_2][\text{PF}_6]_2$ with $\text{CuCl}_2\cdot 2\text{H}_2\text{O}$ results in the assembly of a 2-dimensional network with copper(II) centres coordinated to the pyrimidinyl N-donors [13]. Recently, Granifo et al [14] have reported the synthesis of ligand **2** and shown that it

reacts with $\text{Zn}(\text{acac})_2$ (Hacac = acetylacetonate) to give the discrete complex $[\text{Zn}(\text{acac})_2(\mathbf{2})_2]$, in addition to the 1-dimensional coordination polymer $[\{\text{Zn}(\text{acac})_2(\mathbf{2})\}_n]$. In $[\text{Zn}(\text{acac})_2(\mathbf{2})_2]$, each ligand $\mathbf{2}$ is monodentate and binds through one pyridyl unit, while in $[\{\text{Zn}(\text{acac})_2(\mathbf{2})\}_n]$, each molecule of $\mathbf{2}$ bridges two zinc(II) centres and coordinates through the nitrogen donors of one pyridyl and one pyrimidinyl unit. These results contrast with our own observations on the coordination behaviour of ligands $\mathbf{3}$ and $\mathbf{4}$, described in this work.



Scheme 1. Ligand structures and atom numbering for NMR spectroscopic assignments.

2. Experimental

2.1 General

^1H and ^{13}C NMR spectra were recorded on a Bruker Avance III-500 spectrometer with chemical shifts referenced to residual solvent peaks ($\delta(\text{TMS}) = 0$ ppm). Solution electronic absorption spectra were recorded on a Cary 5000 spectrophotometer. Electrospray ionization (ESI) mass spectra were recorded on a Bruker esquire 3000^{plus} mass spectrometer.

Pyrimidine-5-carbaldehyde (Alfa Aesar) and 2-methylpyrimidine-5-carbaldehyde (Fluorochem) were used as received.

2.2 Ligand 3

Pyrimidine-5-carbaldehyde (0.28 g, 2.5 mmol) was dissolved in EtOH (40 mL) and 4-acetylpyridine (0.57 mL, 0.62 g, 5 mmol) was added, followed by crushed KOH (0.28 g, 5 mmol). The initially colorless solution changed to yellow and then red. Aqueous NH₃ (25% in water, 12.3 mL, 80 mmol) was added dropwise and the reaction mixture stirred at room temperature overnight. A yellow precipitate formed which was collected by filtration, washed with water (3 × 5 mL) and EtOH (3 × 5 mL) and recrystallized from CHCl₃/MeOH. Compound **3** was obtained as a yellow solid (0.34 g, 1.28 mmol, 51%). Decomp. > 260 °C. ¹H NMR (500 MHz, CDCl₃) δ / ppm 9.39 (s, 1H, H^{C2}) 9.13 (s, 2H, H^{C4}), 8.83 (m, 4H, H^{A2}), 8.09 (m, 4H, H^{A3}), 8.04 (s, 2H, H^{B3}). ¹H NMR (500 MHz, *d*-TFA) δ / ppm 9.97 (s, 2H, H^{C4}) 9.80 (s, 1H, H^{C2}), 9.06–8.90 (m, 8H, H^{A2}/H^{A3}), 8.83 (s, 2H, H^{B3}); ¹³C{¹H} NMR (126 MHz, *d*-TFA) δ / ppm 158.4 (C^{C3}), 157.0 (C^{A4}), 155.2 (C^{B2}), 154.5 (C^{C2}), 145.0 (C^{B4}), 144.1 (C^{A2}), 135.8 (C^{C5}), 127.3 (C^{A3}), 125.5 (C^{B3}); IR (solid, ν / cm⁻¹) 4696 (m), 3033 (w), 2925 (w), 1652 (w), 1613 (w), 1596 (s), 1569 (s), 1553 (s), 1544 (m), 1539 (m), 1533 (m), 1506 (w), 1436 (s), 1416 (m), 1393 (s), 1356 (m), 1327 (w), 1318 (w), 1274 (w), 1189 (m), 1133 (w), 1059 (w), 1029 (w), 995 (m), 897 (w), 890 (w), 841 (m), 823 (s), 804 (w), 722 (s), 701 (m), 642 (m), 638 (s), 625 (s), 619 (s), 616 (s), 609 (m), 514 (m), 508 (s), 502 (s). UV-VIS (CH₂Cl₂, 2.5 × 10⁻⁵ M) λ/nm (ε/ dm³ mol⁻¹ cm⁻¹) 242 (47359), 312 (9184). ESI MS *m/z* 312.2 [M+H]⁺ (calc. 312.1). Satisfactory elemental analysis could not be obtained (see text).

2.3 Ligand 4

2-Methylpyrimidine-5-carbaldehyde (0.27 g, 2.21 mmol) was dissolved in EtOH (40 mL), and 4-acetylpyridine (0.57 mL, 0.62 g, 5 mmol) was added followed by crushed solid KOH (0.33 g, 5.90 mmol) after which the solution turned red. Aqueous NH₃ (25% in water, 13.9 mL, 90 mmol) was added dropwise and the mixture stirred overnight at ambient temperature. A yellow precipitate formed which was separated by filtration, washed with water (3 × 7 mL) and ethanol (3 × 7 mL) and recrystallized from chloroform/methanol. Compound **4** was obtained as a white solid (0.26 g, 0.78 mmol, 32%). Decomposition > 260 °C. ¹H NMR (500 MHz, CDCl₃) δ / ppm 9.02 (s, 2H, H^{C4}), 8.83 (m, 4H, H^{A2}), 8.09 (m, 4H, H^{A3}), 8.01 (s, 2H, H^{B3}), 2.87 (s, 3H, H^{Me}); ¹³C {¹H} NMR (126 MHz, CDCl₃) δ / ppm 169.3 (C^{C2}), 155.9 (C^{A4}), 155.14 (C^{C4}), 150.8 (C^{B4}) 150.7 (C^{A2}), 145.3 (C^{B2}), 128.5 (C^{C5}), 121.1 (C^{A3}), 118.3 (C^{B3}), 25.9 (C^{Me}); IR (solid, ν / cm⁻¹) 3077 (w), 3033 (w), 1609 (m), 1594 (s), 1569 (m), 1549 (m), 1544 (m), 1539 (m), 1531 (m), 1464 (s), 1461 (s), 1456 (s), 1447 (m), 1432 (m), 1429 (m), 1423 (m), 1404 (m), 1377 (m), 1373 (m), 1368 (m), 1247 (m), 1064 (m), 1028 (m), 999 (m), 995 (m), 895 (m), 851 (m), 844 (m), 835 (s), 791 (m), 739 (m), 731 (m), 670 (m), 664 (m), 649 (m), 637 (s), 629 (s), 619 (m), 616 (m), 604 (m), 597 (m), 582 (m), 570 (m), 564 (m), 543 (m), 541 (m), 535 (m), 528 (m), 523 (m), 519 (m), 513 (s), 506 (s), 502 (s). UV-VIS (MeCN, 2.5 × 10⁻⁵ M) λ/nm (ε/ dm³ mol⁻¹ cm⁻¹) 247 (44458), 312 (7856). ESI-MS *m/z* 326.3 [M+H]⁺ (calc. 326.1). Found C 69.04, H 4.75, N 20.22; required for C₂₀H₁₅N₅·H₂O C 69.96, H 4.99, N 20.40.

2.4 [*ZnCl*₂(**3**)]_{*n*}

A solution of ZnCl₂ (3.41 mg, 0.025 mmol) in MeOH (8 mL) was layered over a CHCl₃ solution (5 mL) of **3** (7.78 mg, 0.025 mmol) and the tube was sealed with Parafilm.

Colourless crystals of [$\{\text{ZnCl}_2(\mathbf{3})\}_n$] (7.0 mg, 0.016 mmol, 63%) were obtained after 2 weeks. IR (solid, ν / cm^{-1}) 3062 (m), 1615 (s), 1607 (s), 1572 (m), 1559 (m), 1543 (m), 1506 (m), 1447 (m), 1425 (m), 1396 (s), 1323 (m), 1218 (m), 1195 (m), 1135 (w), 1064 (s), 1029 (s), 990 (w), 891 (w), 874 (m), 836 (s), 744 (w), 714 (s), 666 (w), 648 (s), 629 (s), 514 (m). Found C 49.59, H 3.03, N 14.97; required for $\text{C}_{19}\text{H}_{13}\text{N}_5\text{Cl}_2\text{Zn}\cdot\text{H}_2\text{O}$ C 49.01, H 3.25, N 15.04.

2.5 [$\{\text{ZnI}_2(\mathbf{3})\}_n$]

An MeOH (8 mL) solution of ZnI_2 (8.0 mg, 0.025 mmol) was layered over a CHCl_3 (5 mL) solution of $\mathbf{3}$ (7.78 mg, 0.025 mmol). The tube was sealed with Parafilm and after 2 weeks, yellow crystals of [$\{\text{ZnI}_2(\mathbf{3})\}_n$] (3.5 mg, 0.006 mmol, 22%) had grown. IR (solid, ν / cm^{-1}) 3056 (w), 1614 (s), 1606 (s), 1568 (m), 1556 (m), 1506 (w), 1444 (m), 1421 (m), 1396 (s), 1322 (w), 1220 (m), 1192 (w), 1135 (w), 1066 (s), 1025 (s), 991 (w), 886 (w), 873 (w), 851 (m), 836 (s), 746 (w), 717 (m), 668 (w), 648 (s), 634 (s), 626 (s). Found C 35.60, H 2.27, N 10.89; required for $\text{C}_{19}\text{H}_{13}\text{I}_2\text{N}_5\text{I}_2\text{Zn}\cdot\text{H}_2\text{O}$ C 35.19, H 2.33, N 10.80.

2.6 [$\{\text{ZnI}_2(\mathbf{4})\cdot\text{MeOH}\}_n$]

A solution of ZnI_2 (8.0 mg, 0.025 mmol) in MeOH (8 mL) was layered on top of a solution of $\mathbf{3}$ (4.07 mg, 0.013 mmol) in CHCl_3 (5 mL) and the tube was left sealed with Parafilm. Yellow crystals of [$\{\text{ZnI}_2(\mathbf{4})\cdot\text{MeOH}\}_n$] (8.0 mg, 0.012 mmol, 91%) were obtained after 2 weeks. IR (solid, ν / cm^{-1}) 2922 (m), 1608 (s), 1548 (m), 1460 (s), 1406 (m), 1372 (m), 1221 (w), 1065 (m), 1024 (s), 871 (w), 836 (s), 750 (w), 686 (m), 645 (s), 630 (s), 599 (w), 505 (w). Found C 38.11, H 2.95, N 10.50; required for $\text{C}_{20}\text{H}_{15}\text{I}_2\text{N}_5\text{Zn}\cdot\text{MeOH}$ C 37.28, H 2.83, N 10.35.

2.7 Crystallography: general

X-ray quality crystals of the complexes were selected from the bulk samples. Data were collected on a Bruker-Nonius Kappa APEX diffractometer; data reduction, solution and refinement used APEX2 [15] and SHELX13 [16]. The ORTEP plot was produced with Mercury v. 3.2 or 3.3 [17,18] which was also used for structure analysis. Crystallographic data are listed in Table 1.

Table 1. Crystallographic data for compound **4** and the polymers [$\{\text{ZnCl}_2(\mathbf{3})\}_n$], [$\{\text{ZnI}_2(\mathbf{3})\}_n$] and [$\{\text{ZnI}_2(\mathbf{4})\} \cdot \text{MeOH}\}_n$].

Compound	4	[$\{\text{ZnCl}_2(\mathbf{3})\}_n$]	[$\{\text{ZnI}_2(\mathbf{3})\}_n$]	[$\{\text{ZnI}_2(\mathbf{4})\} \cdot \text{MeOH}\}_n$]
Formula	$\text{C}_{20}\text{H}_{15}\text{N}_5$	$\text{C}_{19}\text{H}_{13}\text{Cl}_2\text{N}_5\text{Zn}$	$\text{C}_{19}\text{H}_{13}\text{I}_2\text{N}_5\text{Zn}$	$\text{C}_{21}\text{H}_{19}\text{I}_2\text{N}_5\text{OZn}$
Formula weight	325.37	447.63	630.53	676.58
Crystal colour and habit	colourless block	colourless needle	yellow block	yellow block
Crystal system	orthorhombic	monoclinic	monoclinic	monoclinic
Space group	$Pmn2_1$	$P2_1/n$	$P2_1/n$	$P2_1/n$
$a, b, c / \text{\AA}$	18.0817(12) 4.3834(3) 9.7540(6)	8.4559(11) 19.194(2) 11.2787(13)	10.0386(7) 11.2543(8) 18.3065(13)	11.3508(4) 11.6668(4) 17.6152(6)
$\alpha, \beta, \gamma / ^\circ$	90 90 90	90 97.057(9) 90	90 103.838(3) 90	90 103.204(2) 90
$U / \text{\AA}^3$	773.10(9)	1816.6(4)	2008.2(2)	2271.07(14)
$D_c / \text{Mg m}^{-3}$	1.398	1.637	2.085	1.979
T / K	123	123	123	123
Z	2	4	4	4
$\mu(\text{Cu-K}\alpha) / \text{mm}^{-1}$	0.691	4.701	25.948	23.030
Refln. collected (R_{int})	9665 (0.0295)	15849 (0.0643)	36476 (0.0436)	33192 (0.0387)
Unique refln.	1449	3260	3628	4126
Refln. for refinement	1429	2331	3516	3891
Parameters	121	281	244	274
Threshold	$I > 2\sigma(I)$	$I > 2\sigma(I)$	$I > 2\sigma(I)$	$I > 2\sigma(I)$
$R1$ ($R1$ all data)	0.0262 (0.0265)	0.0528 (0.0795)	0.0272 (0.0283)	0.0222 (0.0237)
$wR2$ ($wR2$ all data)	0.0731 (0.0736)	0.1330 (0.1473)	0.0710 (0.0718)	0.0578 (0.0588)
Goodness of fit	1.088	1.015	1.104	1.035

3 Results and discussion

3.1 Synthesis and characterization of compounds **3** and **4**.

Compounds **3** and **4** were synthesized using the one-pot strategy introduced by Hanan [19] and were isolated in 51 and 32% yields, respectively. The electrospray mass spectrum of **3** and **4** showed base peaks at $m/z = 312.2$ and 326.3 , respectively, arising

from $[M+H]^+$ ions. Satisfactory elemental analytical data for **3** could not be obtained, despite repeated recrystallizations of the bulk material from MeOH/CHCl₃. The ¹H NMR spectrum of a CDCl₃ solution of **3** was assigned using NOESY with observations of cross peaks between signals for H^{C4}/H^{B3} and H^{A3}/H^{B3}. However, the poor solubility of **3** in CDCl₃ (and also in CD₂Cl₂, CD₃CN, CD₃OD and *d*₆-DMSO) did not permit the ¹³C NMR spectrum to be resolved, despite the use of HMQC and HMBC methods. Thus, the ¹H and ¹³C NMR spectra of the protonated ligand were recorded in *d*-TFA and were assigned by 2D methods (COSY, HMQC, HMBC and NOESY). The shifting of all ¹H NMR signals to higher frequency on going from CDCl₃ to *d*-TFA is consistent with multiple protonation of **3** in TFA. Introduction of the 2-methyl-substituent on going from **3** to **4** improves the solubility in CDCl₃.

The absorption spectra of CH₂Cl₂ solutions (2.5×10^{-5} mol dm⁻³) of both **3** and **4** are similar. Intense, high energy bands ($\lambda_{\text{max}} = 242$ nm for **3** and 247 for **4**) and a lower intensity absorption at 312 nm in both compounds were assigned to $\pi^* \leftarrow \pi$ and $\pi^* \leftarrow n$ transitions.

X-ray quality single crystals of **4** were grown serendipitously during attempts to react **4** with iron(II) perchlorate in MeOH; Figure 1 depicts the molecular structure of **4**. The compound crystallizes in the orthorhombic *Pmn*2₁ space group with half the molecular in the asymmetric unit; the second half is generated by a mirror plane. Bond distances and angles (caption to figure 1) are as expected. The planes containing pyridine rings with N1 and N2 lie at 4.5° with respect to each other, and essentially, the molecule is planar. Molecules of **4** engage in face-to-face π -interactions. Adjacent molecules are slipped with respect to one another leading to the dominant interaction being between central pyridine and pyrimidine rings (Figure 2a, distance between planes = 3.32 Å; inter-

centroid separation = 3.63 Å). The stacks assemble in a herring-bone arrangement with CH...N hydrogen bonds as the dominant packing interactions ($C10H10a...N1^{ii} = 2.52$, $C4H4a...N1^{ii} = 2.66$, $C7H7a...N1^{ii} = 2.74$, $N3...H5a^{iii}C5^{iii} = 2.52$ Å, symmetry codes: $ii = \frac{3}{2}-x, 1-y, -\frac{1}{2}+z$; $iii = \frac{3}{2}-x, 2-y, \frac{1}{2}+z$).

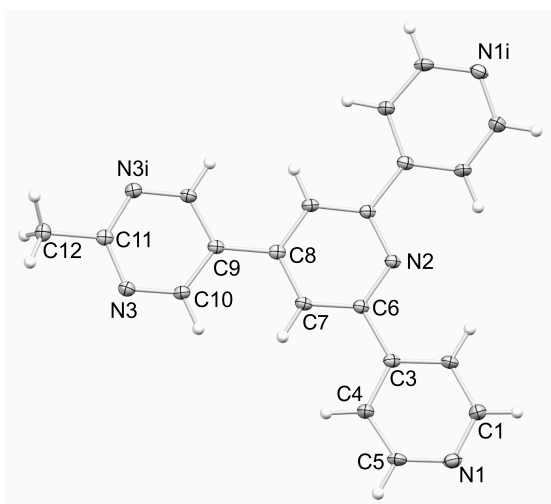


Fig. 1. Structure of molecule **4** with ellipsoids plotted at the 40% probability level. Symmetry code $i = 2-x, y, z$. Selected bond parameters: $N1-C5 = 1.335(2)$, $N1-C1 = 1.337(2)$, $N2-C6 = 1.3402(19)$, $N3-C10 = 1.336(2)$, $N3-C11 = 1.3395(17)$ Å; $C5-N1-C1 = 116.12(15)$, $C6-N2-C6^i = 118.19(19)$, $C10-N3-C11 = 116.69(14)^\circ$.

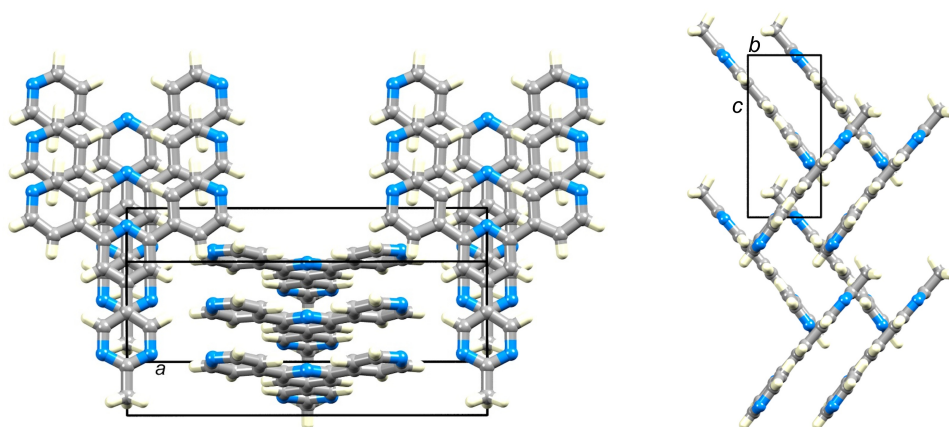


Fig. 2 Packing of molecules of **4** in the crystal lattice showing π -stacking of planar molecules and herring-bone arrangement of the stacks.

3.2 Reaction of **3** with $ZnCl_2$

Layering solutions of MeOH/ $ZnCl_2$ and $CHCl_3$ /**3** resulted in the growth of colourless crystals. Elemental analysis of the bulk sample was consistent with a stoichiometry $ZnCl_2(\mathbf{3})$ and single crystal X-ray analysis confirmed the formation of the 1-dimensional coordination polymer $[\{ZnCl_2(\mathbf{3})\}_n]$. The complex crystallizes in the monoclinic space group $P2_1/n$ with one $\{ZnCl_2(\mathbf{3})\}$ unit in the asymmetric unit. The pyrimidin-5-yl substituent is disordered and has been modelled over two sites (0.61 and 0.39 fractional occupancies) both having atoms C17 and C19 in common. Only the major occupancy site is shown in Figure 3. The rings containing N1, N2 and N3 are essentially coplanar (angles between the planes containing N1/N2 and N2/N3 = 1.8 and 5.3°, respectively); for the major occupancy site, the plane of the pyrimidine ring is twisted 19.8° with respect to the ring containing N3. Atom Zn1 is in a distorted tetrahedral environment and ligand **3** bridges through the outer pyridine rings (N1 and N3) between pairs of $ZnCl_2$ units. As is characteristic of 4,2':6',4"-tpy ligands [1], the central donor N2 is not coordinated. Atoms N4 and N5 in the pyrimidine ring are also non-coordinating. In this respect, the structure can be compared with that of the 1-dimensional polymer $[\{ZnCl_2(4'-(4\text{-pyridyl})-4,2':6',4''\text{-tpy})\}_n]$ [20] in which the pendant pyridyl domain does not coordinate. The structures of $[\{ZnCl_2(\mathbf{3})\}_n]$ and $[\{ZnCl_2(4'-(4\text{-pyridyl})-4,2':6',4''\text{-tpy})\}_n]$ are also similar in that the polymer chains are both built up by 2-fold screw axes. That **3** bridges through two pyridyl donors of the 4,2':6',4"-tpy domain contrasts with the related ligand **2** (Scheme 1) which can bridge through one pyridyl donor and one pyrimidinyl unit [14]. The pitch of the helical $[\{ZnCl_2(\mathbf{3})\}_n]$ chain (19.194(2) Å) is related to the N–Zn–N angle [1] and the value of 107.15(15)° in $[\{ZnCl_2(\mathbf{3})\}_n]$ is similar to that in $[\{ZnCl_2(4'-(4\text{-pyridyl})-4,2':6',4''\text{-tpy})\}_n]$ (108.3(1)°) in which the helical pitch is 20.661(3) Å [20].

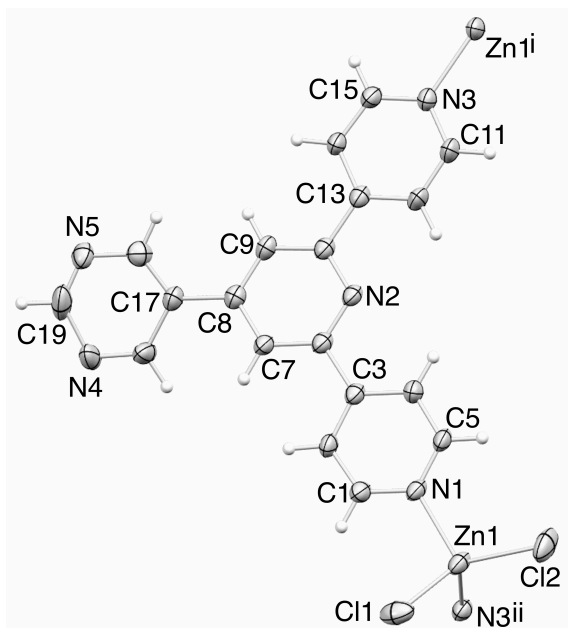


Fig. 3 Repeat unit (showing connectivities to the next units) in $[\{\text{ZnCl}_2(\mathbf{3})\}_n]$; symmetry codes: $i = \frac{1}{2}-x, -\frac{1}{2}+y, \frac{3}{2}-z$; $ii = \frac{1}{2}-x, \frac{1}{2}+y, \frac{3}{2}-z$ and ellipsoids plotted at the 40% probability level. Selected bond parameters: $\text{Zn1-N1} = 2.046(3)$, $\text{Zn1-N3}^{ii} = 2.054(4)$, $\text{Zn1-Cl2} = 2.1996(15)$, $\text{Zn1-Cl1} = 2.2384(17)$ Å; $\text{N1-Zn1-N3}^{ii} = 107.15(15)$, $\text{N1-Zn1-Cl2} = 111.25(12)$, $\text{N3}^{ii}-\text{Zn1-Cl2} = 110.22(11)$, $\text{N1-Zn1-Cl1} = 103.37(12)$, $\text{N3}^{ii}-\text{Zn1-Cl1} = 101.46(12)$, $\text{Cl2-Zn1-Cl1} = 122.15(8)^\circ$.

Both the *P*- and *M*-helices are present in the lattice of $[\{\text{ZnCl}_2(\mathbf{3})\}_n]$ and chains of opposite chirality associate through face-to-face π -interactions of 4,2':6',4''-tpy units. Figure 4 shows that this involves discrete tetradecker domains. At the centre of the sandwich, the rings containing N1 and N2 of a centrosymmetric pair of 4,2':6',4''-tpy units stack with an interplane separation of 3.35 Å. The outer π -interactions involve stacking of the ring with N3 over the pair of rings with N1/N2. The interactions between *P*- and *M*-chains is closely related to that observed in $[\{\text{ZnCl}_2(4'-(4\text{-pyridyl})-4,2':6',4''\text{-tpy})\}_n]$ [1,20].

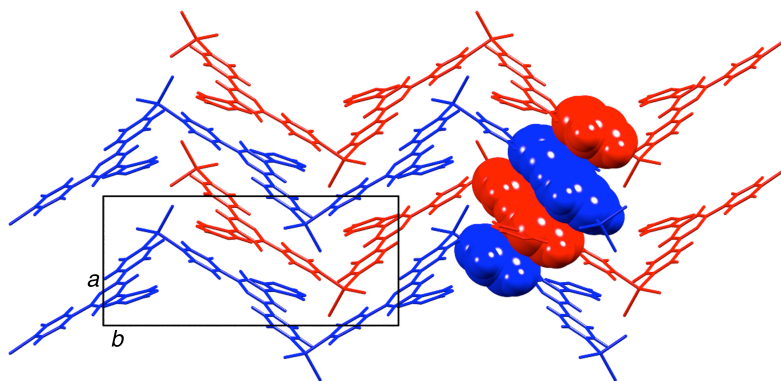


Fig. 4 Packing of *P*- and *M*-chains in $[\{\text{ZnCl}_2(\mathbf{3})\}_n]$ involves discrete tetradecker π -stacking domains involving 4,2':6',4''-tpy units. Chains of opposite chirality are shown in red and blue, respectively.

3.3 Reactions of **3** and **4** with ZnI_2 .

Layering experiments with an MeOH solution of ZnI_2 and CHCl_3 solution of **3** or **4** resulted in the formation of yellow crystals of the 1-dimensional coordination polymers $[\{\text{ZnI}_2(\mathbf{3})\}_n]$ and $[\{\text{ZnI}_2(\mathbf{4})\cdot\text{MeOH}\}_n]$, respectively. Despite the presence of solvent molecules in the latter, the two structures are very similar and will be discussed together. Both complexes crystallize in the monoclinic space group $P2_1/n$ and Figure 5 depicts the repeat unit in $[\{\text{ZnI}_2(\mathbf{4})\cdot\text{MeOH}\}_n]$. The same numbering scheme for both compounds has been used and a comparison of important bond parameters is given in Table 2. The tetrahedral coordination environment of Zn1 in each complex is similarly distorted, as indicated by the N–Zn–N and I–Zn–I bond angles (Table 2). Figure 5 includes the MeOH molecule which forms an O–H...N hydrogen bond with the pyrimidinyl unit ($\text{O100H100...N5} = 2.03$, $\text{O100...N5} = 2.856(3)$ Å, $\text{O100–H100...N5} = 169^\circ$). Its presence in the lattice is associated with an enlarged cavity which results from the replacement of the hydrogen atom attached to C19 in **3** by the methyl group in **4**. The pyridine and pyrimidine rings are twisted with respect to one another in both $[\text{ZnI}_2(\mathbf{3})]_n$ and $[\{\text{ZnI}_2(\mathbf{4})\cdot\text{MeOH}\}_n]$ with twist angles in the range 17.2 to 39.7°.

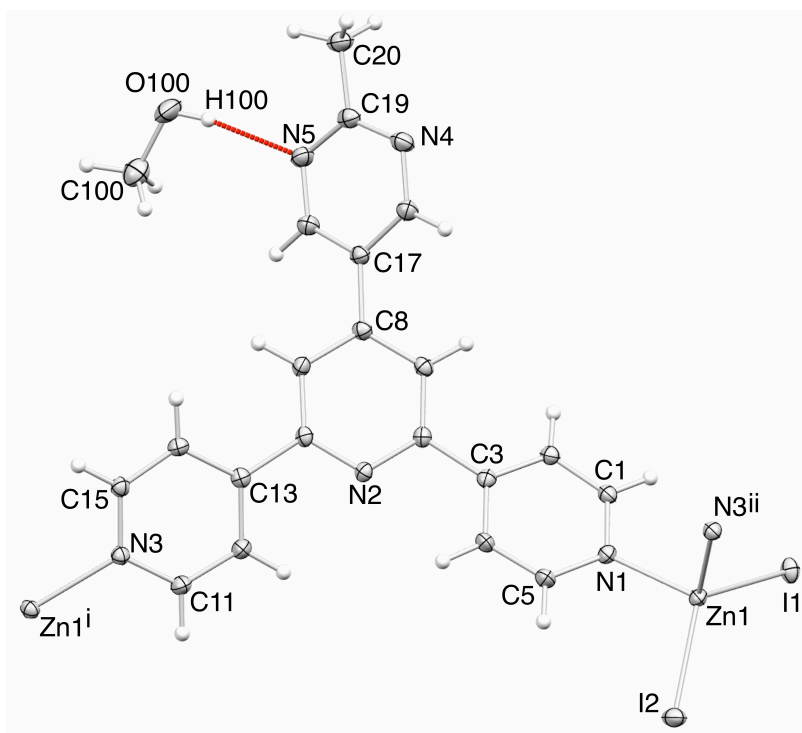


Fig. 5 Repeat unit (showing connectivities to the next units) in $[\{\text{ZnI}_2(\mathbf{4})\cdot\text{MeOH}\}_n]$; symmetry codes: $i = -1/2+x, 1/2-y, -1/2+z$; $ii = 1/2+x, 1/2-y, 1/2+z$) and ellipsoids plotted at the 40% probability level.

Table 2 Comparison of selected bond parameters in $[\{\text{ZnI}_2(\mathbf{3})\}_n]$ and $[\{\text{ZnI}_2(\mathbf{4})\cdot\text{MeOH}\}_n]$. The atom numbering for both complexes is as given in Figure 5.

Bond distance / Å	$[\{\text{ZnI}_2(\mathbf{3})\}_n]^a$	$[\{\text{ZnI}_2(\mathbf{4})\cdot\text{MeOH}\}_n]^b$
Zn–N1	2.065(3)	2.076(2)
Zn1–N3 ⁱⁱ	2.066(3)	2.066(2)
Zn1–I1	2.5376(5)	2.5530(4)
Zn1–I2	2.5324(5)	2.5426(4)
Bond angle / deg		
N1–Zn1–N3 ⁱⁱ	95.54(12)	96.60(9)
I2–Zn1–I1	119.041(19)	123.725(15)

^a Symmetry code: $ii = 1/2+x, 1/2-y, 1/2+z$.

^b Symmetry code: $ii = -1/2+x, 1/2-y, -1/2+z$.

As in $[\{\text{ZnCl}_2(\mathbf{3})\}_n]$, only the outer pyridine rings of the 4,2':6',4''-tpy domains in $[\{\text{ZnI}_2(\mathbf{3})\}_n]$ and $[\{\text{ZnI}_2(\mathbf{4})\cdot\text{MeOH}\}_n]$ bind to zinc(II). In both compounds, the polymer chain is built up along a glide plane, leading to non-helical polymer chains in contrast to that in $[\{\text{ZnCl}_2(\mathbf{3})\}_n]$. The Zn...Zn separations between pairs of adjacent Zn atoms long the chain are 12.9298(9) Å in $[\{\text{ZnI}_2(\mathbf{3})\}_n]$ and 13.0295(6) Å in $[\{\text{ZnI}_2(\mathbf{4})\cdot\text{MeOH}\}_n]$.

Chains in $[\{\text{ZnI}_2(\mathbf{3})\}_n]$ interact with one another through π -interactions between 4,2':6',4''-tpy domains as shown in Figure 6a. This results in the assembly of sheets which slice obliquely through the unit cell (Figure 6b). The pyrimidin-5-yl domains project from each side of the sheet and assist in locking the sheets together in the lattice. Similar packing motifs are present in $[\{\text{ZnI}_2(\mathbf{4})\cdot\text{MeOH}\}_n]$.

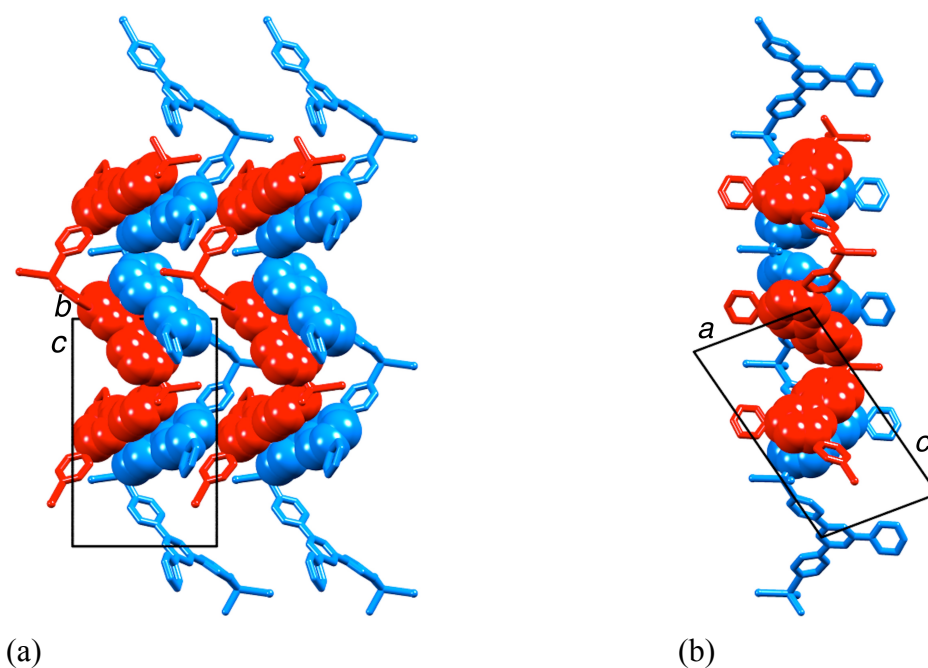


Figure 6. Assembly of sheets of chains in $[\{\text{ZnI}_2(\mathbf{3})\}_n]$. (a) View down the *a*-axis to emphasize the face-to-face π -interactions between chains, and (b) view down the *b*-axis showing the protruding pyrimidin-5-yl domains on each side of the sheet.

3.4 Solution absorption spectra of the coordination polymers

The absorption spectra of MeCN solutions of dissolved crystalline [$\{\text{ZnCl}_2(\mathbf{3})\}_n$] and [$\{\text{ZnI}_2(\mathbf{3})\}_n$] both showed a broad maximum at 242 nm with a lower energy shoulder at \approx 310 nm. The spectra are very similar to that of an MeCN solution of free ligand **3**. The absorption spectra of MeCN solutions of [$\{\text{ZnI}_2(\mathbf{4})\}_n$] and **4** both exhibit the same band maxima at 247 and 312 nm. The data are consistent with dissociation of the complexes in MeCN solution, thus precluding further solution characterization of the materials.

4 Conclusions

We have described the preparation and characterization of two new 4'-functionalized 4,2':6',4''-tpy ligands bearing pendant pyrimidin-5-yl or 2-methylpyrimidin-5-yl substituents. In reactions with ZnCl_2 and ZnI_2 , the ligands bind only through the outer pyridine donors and form 1-dimensional coordination polymers [$\{\text{ZnCl}_2(\mathbf{3})\}_n$], [$\{\text{ZnI}_2(\mathbf{3})\}_n$] and [$\{\text{ZnI}_2(\mathbf{4})\cdot\text{MeOH}\}_n$]. [$\{\text{ZnCl}_2(\mathbf{3})\}_n$] is helical and crystallizes as a racemate; it is structurally similar to the previously reported [$\{\text{ZnCl}_2(4'-(4\text{-pyridyl})-4,2':6',4''\text{-tpy})\}_n$] [20]. In contrast, the chains in [$\{\text{ZnI}_2(\mathbf{3})\}_n$] and [$\{\text{ZnI}_2(\mathbf{4})\cdot\text{MeOH}\}_n$] are built up by glide planes. The two compounds are structurally analogous, and chains pack into sheets through π -interactions between 4,2':6',4''-tpy domains; the pyrimidin-5-yl units protrude from the sheets and are involved in interlocking the latter into a 3D assembly. Introducing the 2-methyl substituent on going from **3** to **4** pushes the sheets apart slightly, resulting in MeOH solvent molecules being accommodated in cavities between the layers.

Acknowledgements

We thank the Swiss National Science Foundation and the University of Basel for financial support, and acknowledge additional laboratory support from Srboľjub Vujovic.

Appendix 1 Supplementary data

Crystallographic data have been deposited with the CCDC (Cambridge Crystallographic Data Centre, 12 Union Road, Cambridge CB2 1EZ, UK; fax +44 1223 336033; e-mail: deposit@ccdc.cam.ac.uk or www: <http://www.ccdc.cam.ac.uk>) and may be obtained free of charge on quoting the deposition numbers CCDC 996287–996290.

References

- 1 C. E. Housecroft, Dalton Trans. 43 (2014) 6594
- 2 M. Barquín, J. Cancela, M. J. González Garmendia, J. Quintanilla, U. Amador, Polyhedron 17 (1998) 2373.
- 3 E. C. Constable, C. E. Housecroft, P. Kopecky, M. Neuburger, J. A. Zampese, G. Zhang, CrystEngComm 14 (2012) 446.
- 4 L. Hou, D. Li, Inorg. Chem. Comm. 8 (2005) 190.
- 5 X.-Z. Li, M. Li, Z. Li, J.-Z. Hou, X.-C. Huang, D. Li, Angew. Chem. Int. Ed. 47 (2008) 6371.
- 6 G. W. V. Cave, C. L. Raston, J. Supramol. Chem. 2 (2002) 317.
- 7 E. C. Constable, G. Zhang, C. E. Housecroft, J. A. Zampese, CrystEngComm 13 (2011) 6864.
- 8 J. Heine, J. Schmedt auf der Günne, S. Dehnen, J. Am. Chem. Soc. 133 (2011) 10018.
- 9 F. Yuan, Q.-E. Zhu, H.-M. Hu, J. Xie, B. Xu, C.-M. Yuan, M.-L. Yang, F.-X. Dong, G.-L. Xue, Inorg. Chim. Acta 397 (2013) 117.

-
- 10 H.-N. Zhang, F. Yuan, H.-M. Hu, S.-S. Shen, G.-L. Xue, *Inorg. Chem. Comm.* 34 (2013) 51.
 - 11 Y.-L. Gai, F.-L. Jiang, L. Chen, Y. Bu, M.-Y. Wu, K. Zhou, J. Pan, M.-C. Hong, *Dalton's Trans.* 42 (2013) 9954.
 - 12 E. C. Constable, C. E. Housecroft, S. Vujovic, J. A. Zampese, *CrystEngComm* 16 (2014) 3494.
 - 13 J. E. Beves, E. C. Constable, S. Decurtins, E. L. Dunphy, C. E. Housecroft, T. D. Keene, M. Neuburger, S. Schaffner, *CrystEngComm* 10 (2008) 986.
 - 14 J. Granifo, R. Gaviño, E. Freire, R. Baggio, *J. Mol. Struct.* 1063 (2104) 102.
 - 15 Bruker Analytical X-ray Systems, Inc., 2006, APEX2, version 2 User Manual, M86-E01078, Madison, WI.
 - 16 G. M. Sheldrick, *Acta Crystallogr., Sect. A*, 64 (2008) 112.
 - 17 I. J. Bruno, J. C. Cole, P. R. Edgington, M. K. Kessler, C. F. Macrae, P. McCabe, J. Pearson, R. Taylor, *Acta Crystallogr., Sect. B*, 58 (2002) 389.
 - 18 C. F. Macrae, I. J. Bruno, J. A. Chisholm, P. R. Edgington, P. McCabe, E. Pidcock, L. Rodriguez-Monge, R. Taylor, J. van de Streek, P. A. Wood, *J. Appl. Cryst.*, 41 (2008) 466.
 - 19 J. Wang, G. S. Hanan, *Synlett* (2005) 1251.
 - 20 B.-C. Wang, Q.-R. Wu, H.-M. Hu, X.-L. Chen, Z.-H. Yang, Y.-Q. Shangguan, M.-L. Yang and G.-L. Xue, *CrystEngComm* 12 (2010) 485.